# Optimal Adaptive Power Flow Linearizations: Expected Error Minimization using Polynomial Chaos Expansion

Tillmann Mühlpfordt*, Daniel K. Molzahn†, Veit Hagenmeyer*, and Sidhant Misra‡
*Karlsruhe Institute of Technology, Germany, {tillmann.muehlpfordt, veit.hagenmeyer}@kit.edu
†Argonne National Laboratory, USA, dmolzahn@anl.gov
‡Los Alamos National Laboratory, USA, sidhant@lanl.gov

***Abstract*—The nonlinearity of the power flow equations leads to algorithmic and theoretical challenges for a wide variety of optimization and control problems relevant to electric power systems. Solution algorithms for these problems often use linearization techniques to obtain tractable power flow formulations. Many existing linearizations lack specialization to a given system and operating range of interest, leading to unnecessarily large linearization errors. In contrast, recently proposed "optimal adaptive" linearizations are 1) tailored to specific systems and operating ranges of interest and 2) optimal in the sense that they minimize a selected error metric relative to the nonlinear power flow equations. Existing work proposes optimal adaptive linearizations that minimize the *worst-case* linearization error. Building on this existing work, this paper uses an uncertainty quantifiation method called Polynomial Chaos Expansion to minimize the *expected* linearization error for a given probability distribution of the power injections. As validated using Monte Carlo analyses, the capabilities of the expected-error-minimizing linearizations are shown to be superior to first-order Taylor approximations computed at a nominal operating point.**

## I. Introduction

The AC power flow equations model the nonlinear relationship between the power injections and the voltage phasors in an electric power system. These equations are at the heart of power system optimization and control problems. Since the nonlinearity of these equations results in both computational and theoretical challenges, many power system algorithms employ linear power flow approximations, such as the DC power flow [1] for transmission systems and the LinDistFlow [2] for distribution systems. There exist many variants of these linearizations as well as other approximation techniques [3].

These linearizations facilitate the use of well-developed theory for linear optimization and linear dynamical systems analysis, often enabling computational scalability to large-scale systems and real-time computations. However, the use of linearizations introduces numerical errors relative to the nonlinear power flow equations, which may cause problems for power system reliability (e.g. an operating point that is predicted to be secure by a linearization may actually result in constraint violations) and economics (e.g. security margins used to account for linearization errors can preclude lower-cost operation). Linearizations with smaller errors can improve reliability and economics while maintaining tractability.

Typical linearizations are designed using assumptions applicable to general classes of systems. For instance, the DC power flow assumes a nearly lossless network operated with small angle differences and near-nominal voltage magnitudes. The linearization errors depend on the appropriateness of the underlying assumptions, which can be difficult to quantify. In contrast, the linearizations proposed in [4] are *adaptive*, i.e., tailored to a specific system and operating range of interest, and *optimal*, i.e., they minimize a certain error metric relative to the nonlinear power flow equations. By exploiting knowledge of specific systems and operating ranges, these "optimal adaptive" linearizations achieve lower errors compared to typical power flow linearization techniques. As a byproduct, algorithms for computing these linearizations also provide error bounds. Optimal adaptive linearizations can be computed off-line based on a forecast and employed in on-line analyses that require fast computations.

These linearizations can replace traditional techniques in order to improve performance in any application that uses power flow linearizations. Several particularly relevant power systems applications include chance-constrained optimization [5, 6], where linear power flow models facilitate uncertainty propagation, and model predictive control [7], where the requirement for fast solutions of multi-period optimization problems is well matched to the optimal adaptive linearizations' capabilities.

The linearizations' characteristics depend on the selected error metric. Two possible metrics are *worst-case* error and *expected* error. The worst-case error results in linearizations that ignore the likelihoods of the uncertainty realizations. However, the likelihoods can be valuable for problems concerned with extreme scenarios. Conversely, an expected error metric considers each realization's likelihood of occurring, which can improve the linearization's accuracy for "typical" operating conditions.

Building on [8], the optimal adaptive linearizations in [4] minimize the worst-case linearization error. To compute these linearizations, a constraint-generation algorithm alternates between 1) computing the power injections that result in the worst-case error for a candidate linearization and 2) updating the candidate linearization in order to reduce the error with respect to all previously calculated worst-case power injections. The works [9, 10] study adaptive linearizations using expected errors. Reference [9] (with extensions to three-phase systems in [11]) minimizes the least-square linearization

error for a predefined set of evenly distributed points near a nominal operating point. While the resulting linearization is *adaptive* to the system and operating range of interest, the set of points is not selected in any *optimal* manner to minimize some objective. Using a "generalized moment" approach, [10] also computes power flow linearizations that minimize the expected error. Specifically, [10] minimizes the error for the *solution* to a specified optimization problem (parameterized by the uncertain power injections).

In contrast, the main contribution of this paper is an approach for computing linearizations that minimize the expected linearization error for a given distribution of uncertain power injections; hence considering an entire operating range, independent of any particular application. The linearizations are calculated using an uncertainty quantification method called *Polynomial Chaos Expansion* (PCE) [12, 13]. PCE can handle many classes of probability distributions and does not require sampling. Prior applications of PCE to power systems include stochastic power flow [14] and chance-constrained optimal power flow [6, 15, 16].

The present paper is organized as follows. Section II poses the problem formulation. Section III proposes our PCE approach for solving this formulation. Section IV numerically demonstrates the advantages of the proposed approach. Section V concludes the paper and discusses future work.

## II. Problem Formulation

After introducing the power flow equations, this section presents the stochastic optimization formulation used to determine the expected-error-minimizing linearizations.

### A. Power Flow Overview

Consider an $n$-bus power system with sets of buses and lines denoted $\mathcal{N}$ and $\mathcal{L}$, respectively. Each line $(j,k) \in \mathcal{L}$ is modeled by a $\Pi$-circuit with shunt susceptance $b_{c,jk}$, mutual conductance $g_{jk}$, and mutual susceptance $b_{jk}$. The active and reactive power flows on each line $(j,k) \in \mathcal{L}$ are $p_{jk}$ and $q_{jk}$. Each bus $i \in \mathcal{N}$ has shunt conductance and susceptance $g_{sh,i}$ and $b_{sh,i}$ as well as active and reactive power injections denoted $P_i$ and $Q_i$. The voltage phasors at bus $i \in \mathcal{N}$ in rectangular coordinates have real part $e_i$ and imaginary part $f_i$. The angle reference is selected by choosing $f_1 = 0$. The power flow equations are, for all $(j,k) \in \mathcal{L}$ and $i \in \mathcal{N}$,

$$p_{jk} = g_{jk}(e_j^2 + f_j^2 - e_j e_k - f_j f_k) + b_{jk}(e_j f_k - f_j e_k), \tag{1a}$$

$$q_{jk} = -(b_{jk} + b_{c,jk}/2)(e_j^2 + f_j^2) - b_{jk}(e_j e_k - f_j f_k) + g_{jk}(e_j f_k - f_j e_k), \tag{1b}$$

$$P_i = \sum_{\substack{(j,k)\in\mathcal{L} \\ \text{s.t. } j=i}} p_{jk} + \sum_{\substack{(j,k)\in\mathcal{L} \\ \text{s.t. } k=i}} p_{kj} + g_{sh,i}(e_i^2 + f_i^2), \tag{1c}$$

$$Q_i = \sum_{\substack{(j,k)\in\mathcal{L} \\ \text{s.t. } j=i}} q_{jk} + \sum_{\substack{(j,k)\in\mathcal{L} \\ \text{s.t. } k=i}} q_{kj} - b_{sh,i}(e_i^2 + f_i^2), \tag{1d}$$

$$v_i^2 = e_i^2 + f_i^2. \tag{1e}$$

Equations (1a) and (1b) relate the voltage phasors to the line flows. Equations (1c) and (1d) correspond to active and reactive power balance at each bus. The squared voltage magnitudes are modeled in (1e).

To represent typical equipment behavior, we choose to specify each bus as "PQ" (fixed active and reactive power injections), "PV" (fixed active power injection and voltage magnitude), or "slack" (fixed voltage magnitude and angle reference, i.e., $f_i = 0$). We define the sets of PQ, PV, and slack buses as $\mathcal{PQ}$, $\mathcal{PV}$, and $\mathcal{S}$, respectively.[1]

Together with the bus type specifications, the power flow equations (1) constitute an implicit nonlinear mapping from $\mathbb{R}^{2n} \to \mathbb{R}^{2n}$. We denote this mapping as $h(P, Q, e, f) = 0$.

### B. Expected Error Minimization Problem Formulation

We seek a linearization that relates a single "output" quantity of interest to some "input" quantities.[2] The output is typically a quantity that is constrained or optimized but not directly controlled, such as voltage magnitudes at PQ buses, active and reactive line flows, and current flows. Typically, the inputs are controllable quantities or uncertain parameters. While the approach we propose is applicable to a variety of choices for input and output quantities, this paper focuses on outputs consisting of active and reactive power flows on each line, $p_{jk}$ and $q_{jk}$, and inputs consisting of active and reactive power injections at each non-slack bus, $P_i$ and $Q_i$, $\forall i \in \mathcal{N} \setminus \mathcal{S}$. This choice of inputs and outputs results in linearizations analogous to commonly used "Power Transfer Distribution Factor" (PTDF) formulations. In fact, shrinking the operating range to a single nominal point results in our proposed linearizations being equivalent to the so-called "AC-PTDF" that uses a first-order Taylor expansion to minimize the linearization error at a nominal operating point [17]. Thus, our proposed linearizations can be interpreted as "adjustments" to an AC-PTDF matrix that account for a range of operation around a nominal point.

Our linearizations are defined by coefficients that form an affine relationship between the input and output quantities. The constant term and the coefficients for active and reactive power injections are denoted as $\ell_0$, $\ell_{Pi}$, and $\ell_{Qi}$, $\forall i \in \mathcal{N} \setminus \mathcal{S}$. We tailor our linearizations to a particular system model with a given network topology and electrical parameters as well as a specific operating range of interest. The operating range is modeled by random variables for the active and reactive power injections with known probability distributions, denoted as $\mathsf{P}_i$, $\forall i \in \mathcal{PQ} \cup \mathcal{PV}$, and $\mathsf{Q}_i$, $\forall i \in \mathcal{PQ}$. While the voltage magnitudes at PV and slack buses can also generally be represented by random variables $\mathsf{v}_i$, $\forall i \in \mathcal{PV} \cup \mathcal{S}$, we consider constant voltage magnitudes at these buses. Each uncertainty realization for these quantities results in a square system of power flow equations $h(\cdot)$ (i.e., equal numbers of equalities and variables). The corresponding "high-voltage" solution to these equations has voltage phasor components $e_i$ and $f_i$ with associated random variables denoted as $\mathsf{e}_i$ and $\mathsf{f}_i$, $\forall i \in \mathcal{N}$.

[1] Our approach admits more general models of equipment behavior, such as "$Q/V$ droop" characteristics, where the generators' reactive power outputs are functions of their voltage magnitudes.

[2] Consequently, if we speak of *linearizations* (plural) we mean the set of mappings that relates *several* outputs to inputs.

Let $\mathbb{E}[\cdot]$ denote the expected value operator. To formalize the optimal adaptive linearization formulation, consider a linearization that relates the active power flow on a specific line $(j,k) \in \mathcal{L}$, $p_{jk}$, to the active and reactive power injections $P_i$ and $Q_i$ at each non-slack bus $i \in \mathcal{N} \setminus \mathcal{S}$:

$$\min_{\ell=[\ell_0,\ell_P,\ell_Q]^\top} \mathbb{E}[(\mathsf{p}_{jk} - \hat{\mathsf{p}}_{jk})^2] \quad \text{subject to} \tag{2a}$$

$$h(\mathsf{P}, \mathsf{Q}, \mathsf{e}, \mathsf{f}) = 0, \tag{2b}$$

$$\mathsf{p}_{jk} = g_{jk}(\mathsf{e}_j^2 + \mathsf{f}_j^2 - \mathsf{e}_j\mathsf{e}_k - \mathsf{f}_j\mathsf{f}_k) + b_{jk}(\mathsf{e}_j\mathsf{f}_k - \mathsf{f}_j\mathsf{e}_k), \tag{2c}$$

$$\hat{\mathsf{p}}_{jk} = \ell_0 + \sum_{i\in\mathcal{N}\setminus\mathcal{S}} (\ell_{Pi}\,\mathsf{P}_i + \ell_{Qi}\,\mathsf{Q}_i), \tag{2d}$$

where $\mathsf{p}_{jk}$ is the random variable corresponding to the active power flow on line $(j,k) \in \mathcal{L}$ and $(\,\cdot\,)^\top$ denotes the transpose. The objective (2a) minimizes the expected squared error between the linearization and the nonlinear power flow equations for this line flow. Constraint (2b) denotes the power flow equations (1) with the bus specifications for the random variables $\mathsf{P}$, $\mathsf{Q}$, $\mathsf{e}$, and $\mathsf{f}$, as discussed above. Constraints (2c) and (2d) model the nonlinear active power flow equation and its linearization, parameterized by the decision variables $\ell = [\ell_0, \ell_P, \ell_Q]^\top$. The decision variables for the solution to (2) give the optimal adaptive linearization's coefficients. The optimal objective value bounds the linearization's expected squared error. Note that linearizations for the active power flows $p_{lm}$ on each line $(l,m) \in \mathcal{L}$ as well as variants of (2) that consider other output quantities of interest (e.g., reactive power flows $q_{lm}$; voltage magnitudes $v_i$, $\forall i \in \mathcal{PQ}$; etc.) are computed in parallel.

## III. Solution Methodology

The linearization problem (2) has finitely many decision variables $\ell$. Nevertheless, this problem is challenging since the power flow equations in terms of random variables (2b) are infinite-dimensional. Additionally, the calculation of the expectation (2a) requires solving an integral. To address these challenges, we exploit the problem's structure, specifically the facts that 1) the active power line flow in (2c) is explicitly determined from the solution to the square system of power flow equations (2b) and 2) the decision variables $\ell$ only appear in (2d). Hence, problem (2) can be decomposed into two steps:

1) *Feasibility problem:* solve the probabilistic power flow problem (2b), i.e., compute the distributions for $\mathsf{e}_i$ and $\mathsf{f}_i$, $\forall i \in \mathcal{N}$; $\mathsf{Q}_i$, $\forall i \in \mathcal{PV} \cup \mathcal{S}$; and $\mathsf{P}_i$, $i \in \mathcal{S}$ given the distributions for $\mathsf{P}_i$, $\forall i \in \mathcal{PV} \cup \mathcal{PQ}$, and $\mathsf{Q}_i$, $\forall i \in \mathcal{PQ}$.
2) *Unconstrained optimization problem:* determine the optimal linearization coefficients $\ell$ by substituting the resulting distributions for $\mathsf{e}_i$, $\mathsf{f}_i$, $\mathsf{P}_i$, and $\mathsf{Q}_i$ into (2c) and (2d) and then minimizing (2a).

Since the probabilistic power flow problem (2b) is independent of the objective (2a), the solution from the first step can be repeatedly used (in parallel) to compute linearizations for multiple quantities of interest in the second step.

Even though we can decompose the linearization problem (2), the probabilistic power flow problem (2b) remains infinite-dimensional and is therefore challenging. Also, the objective (2a) still requires evaluating an integral. We cope with both challenges by means of Polynomial Chaos Expansion (PCE), which is, loosely speaking, a "Fourier series for random variables" [13]. PCE enables any random variable of finite variance to be represented by a set of deterministic scalars, the so-called PCE coefficients. These PCE coefficients are to random variables what Fourier coefficients are to periodic signals: if the PCE (Fourier coefficients) are known, the entire random variable (periodic signal) may be reconstructed. With respect to (2), PCE allows the probabilistic power flow problem to be reformulated as a deterministic system of equations, and the objective (2a) can be formulated entirely in terms of the PCE coefficients. Before presenting these reformulations, we briefly introduce PCE; see [13] for details.

### A. Polynomial Chaos Expansion

Consider a (multivariate) probability density function $\rho : \mathcal{D} \to \mathbb{R}$. Then, there exist polynomials $\{\psi_l\}_{l=0}^{\infty}$ on $\mathcal{D}$ that are orthogonal with respect to the probability density function $\rho$:

$$\langle \psi_k, \psi_l \rangle := \int_{\mathcal{D}} \psi_k(\tau)\psi_l(\tau)\rho(\tau)\mathrm{d}\tau = \gamma_l \delta_{kl}, \tag{3}$$

where $\gamma_l$ is positive and $\delta_{kl}$ is the Kronecker-delta. The truncated polynomial chaos expansion of a random vector $\mathsf{x} = [\mathsf{x}_1, \ldots, \mathsf{x}_n]$ is then

$$\mathsf{x} \approx \sum_{l=0}^{L} \tilde{x}_l \psi_l, \quad \tilde{x}_l = \begin{bmatrix} \frac{\langle \mathsf{x}_1, \psi_l \rangle}{\langle \psi_l, \psi_l \rangle} & \cdots & \frac{\langle \mathsf{x}_n, \psi_l \rangle}{\langle \psi_l, \psi_l \rangle} \end{bmatrix}^\top \in \mathbb{R}^n, \tag{4}$$

hence a weighted sum of basis polynomials. The weight $\tilde{x}_l$ is the vector of so-called PCE coefficients. The components of the truncation error $\mathsf{x} - \sum_{l=0}^{L} \tilde{x}_l \psi_l$ are optimal in the induced norm $\|\cdot\|^2 = \langle \cdot, \cdot \rangle$, and decay to zero for $L \to \infty$. Moments of the random vector $\mathsf{x}$ can be expressed as functions of its PCE coefficients, for example

$$\mathbb{E}[\mathsf{x}] = \tilde{x}_0, \quad \mathbb{E}[\mathsf{x}\mathsf{x}^\top] = \sum_{l=0}^{L} \gamma_l \tilde{x}_l \tilde{x}_l^\top, \tag{5}$$

which follows from orthogonality of the basis, see (3); no sampling is required. The orthogonal basis polynomials are known for certain families of random variables (e.g., Gaussian, Beta, Gamma, and Uniform distributions) [13]. For other random variables, the orthogonal bases $\{\psi_l\}_{l=0}^{\infty}$ can be constructed by the Gram-Schmidt procedure or the Stieltjes procedure [18].

Two aspects of PCE are especially helpful for the linearization problem (2): Galerkin projection for probabilistic power flow (2b) (Section III-B) and computation of moments for the objective (2a) (Section III-C).

### B. Probabilistic Power Flow

We next show how PCE facilitates the reformulation of probabilistic power flow (2b) as a deterministic system of equations in terms of the PCE coefficients, similar to [14]. First, we introduce PCE for all random variables in (2b):

$$h\left(\sum_{l=0}^{L} \tilde{P}_l \psi_l, \sum_{l=0}^{L} \tilde{Q}_l \psi_l, \sum_{l=0}^{L} \tilde{e}_l \psi_l, \sum_{l=0}^{L} \tilde{f}_l \psi_l\right) = 0, \tag{6}$$

$$\tilde{p}_{jk,m} = \sum_{l_1,l_2=0}^{L} \beta_{l_1 l_2 m} \left( g_{jk} \left( \tilde{e}_{j,l_1}\tilde{e}_{j,l_2} + \tilde{f}_{j,l_1}\tilde{f}_{j,l_2} - \tilde{e}_{j,l_1}\tilde{e}_{k,l_2} - \tilde{f}_{j,l_1}\tilde{f}_{k,l_2} \right) + b_{jk} \left( \tilde{e}_{j,l_1}\tilde{f}_{k,l_2} - \tilde{f}_{j,l_1}\tilde{e}_{k,l_2} \right) \right) \tag{8a}$$

$$\tilde{q}_{jk,m} = \sum_{l_1,l_2=0}^{L} \beta_{l_1 l_2 m} \left( -(b_{jk} + b_{c,jk}/2) \left( \tilde{e}_{j,l_1}\tilde{e}_{j,l_2} + \tilde{f}_{j,l_1}\tilde{f}_{j,l_2} \right) - b_{jk} \left( \tilde{e}_{j,l_1}\tilde{e}_{k,l_2} - \tilde{f}_{j,l_1}\tilde{f}_{k,l_2} \right) + g_{jk} \left( \tilde{e}_{j,l_1}\tilde{f}_{k,l_2} - \tilde{f}_{j,l_1}\tilde{e}_{k,l_2} \right) \right) \tag{8b}$$

$$\tilde{P}_{i,m} = \sum_{\substack{(j,k)\in\mathcal{L} \\ \text{s.t. } j=i}} \tilde{p}_{jk,m} + \sum_{\substack{(j,k)\in\mathcal{L} \\ \text{s.t. } k=i}} \tilde{p}_{kj,m} + \sum_{l_1,l_2=0}^{L} \beta_{l_1 l_2 m} g_{sh,i} \left( \tilde{e}_{i,l_1}\tilde{e}_{i,l_2} + \tilde{f}_{i,l_1}\tilde{f}_{i,l_2} \right) \tag{8c}$$

$$\tilde{Q}_{i,m} = \sum_{\substack{(j,k)\in\mathcal{L} \\ \text{s.t. } j=i}} \tilde{q}_{jk,m} + \sum_{\substack{(j,k)\in\mathcal{L} \\ \text{s.t. } k=i}} \tilde{q}_{kj,m} - \sum_{l_1,l_2=0}^{L} \beta_{l_1 l_2 m} b_{sh,i} \left( \tilde{e}_{i,l_1}\tilde{e}_{i,l_2} + \tilde{f}_{i,l_1}\tilde{f}_{i,l_2} \right) \tag{8d}$$

$$\sum_{l_1,l_2=0}^{L} \tilde{v}_{i,l_1}\tilde{v}_{i,l_2} \langle \psi_{l_1}\psi_{l_2}, \psi_m \rangle = \sum_{l_1,l_2=0}^{L} (\tilde{e}_{i,l_1}\tilde{e}_{i,l_2} + \tilde{f}_{i,l_1}\tilde{f}_{i,l_2}) \langle \psi_{l_1}\psi_{l_2}, \psi_m \rangle \tag{8e}$$

$$\forall i \in \mathcal{N}, \quad \forall (j,k) \in \mathcal{L}, \quad \forall m = 0, \ldots, L, \text{ and } \beta_{l_1 l_2 m} = \langle \psi_{l_1}\psi_{l_2}, \psi_m \rangle / \langle \psi_m, \psi_m \rangle$$

where $\tilde{P}_l$, $\tilde{Q}_l$, $\tilde{e}_l$, and $\tilde{f}_l$ are the $l$-th vectors of PCE coefficients of the active and reactive power injections and real and imaginary voltage phasor components, respectively, see (4). We next apply Galerkin projection, i.e., we project every component of (6) onto every basis function $\psi_m$:

$$\left\langle h \left( \sum_{l=0}^{L} \tilde{P}_l \psi_l, \sum_{l=0}^{L} \tilde{Q}_l \psi_l, \sum_{l=0}^{L} \tilde{e}_l \psi_l, \sum_{l=0}^{L} \tilde{f}_l \psi_l \right), \psi_m \right\rangle = 0 \tag{7}$$

for all $m = 0, \ldots, L$.[3] The resulting projected power flow equations are listed in (8). The projected bus specifications are omitted due to space limitations; we refer to equation (12) in [14] for their derivation. Notice that PCE-overloaded power flow from (8) has the same mathematical structure as the deterministic power flow; namely, it is a system of quadratic equations in the real and imaginary voltage PCE coefficients, weighted by the scalar $\beta_{l_1 l_2 m}$ that depends on the basis functions. Values for the scalars $\beta_{l_1 l_2 m}$ are computed offline by Gauss quadrature. Having solved the PCE-overloaded power flow problem, all vectors of PCE coefficients $\tilde{P}_l$, $\tilde{Q}_l$, $\tilde{e}_l$, and $\tilde{f}_l$ are known for $l = 0, \ldots, L$.

### C. Optimal Linearization Coefficients

Turning to the objective (2a), we next show how PCE facilitates the derivation of a closed-form solution in terms of PCE coefficients. We first substitute the equalities (2c) and (2d) into the objective to obtain an unconstrained optimization problem. We then rewrite (2a) as

$$\mathbb{E}[(\mathsf{p}_{jk} - \hat{\mathsf{p}}_{jk})^2] = \mathbb{E}[\hat{\mathsf{p}}_{jk}^2] - 2\mathbb{E}[\mathsf{p}_{jk}\hat{\mathsf{p}}_{jk}] + \mathbb{E}[\mathsf{p}_{jk}^2]. \tag{9}$$

For the first term $\mathbb{E}[\hat{\mathsf{p}}_{jk}^2]$ in (9), we use the ansatz (2d) for the active power flow $\hat{\mathsf{p}}_{jk}$ and compute the moments according to (5). We obtain (recall from (2) that $\ell = [\ell_0, \ell_P, \ell_Q]^\top$)

$$\mathbb{E}[\hat{\mathsf{p}}_{jk}^2] = \ell^\top W \ell, \quad \text{where} \tag{10}$$

$$W = \begin{bmatrix} 1 & t^\top \\ t & T \end{bmatrix}, \; t = \begin{bmatrix} \tilde{P}_0 \\ \tilde{Q}_0 \end{bmatrix}, \; T = \sum_{l=0}^{L} \begin{bmatrix} \tilde{P}_l \tilde{P}_l^\top & \tilde{P}_l \tilde{Q}_l^\top \\ \tilde{Q}_l \tilde{P}_l^\top & \tilde{Q}_l \tilde{Q}_l^\top \end{bmatrix}.$$

Notice that the matrix $W$ is positive (semi)definite. For the second term $\mathbb{E}[\mathsf{p}_{jk}\hat{\mathsf{p}}_{jk}]$ in (9), we substitute (2c) and (2d) and then apply the moment equation (5) to obtain

$$\mathbb{E}[\mathsf{p}_{jk}\hat{\mathsf{p}}_{jk}] = w^\top \ell, \tag{11}$$

[3] We slightly abuse notation since $h$ is vector-valued but the scalar product $\langle \cdot, \cdot \rangle$ is defined in (3) for scalar-valued arguments. Equation (7) takes the scalar product of every component of $h$ with $\psi_m$ for all $m = 0, \ldots, L$.

where the vector $w$ is defined in (12) at the top of the following page. Finally, using (5), the third term $\mathbb{E}[\mathsf{p}_{jk}^2]$ becomes $\mathbb{E}[\mathsf{p}_{jk}^2] = \sum_{l=0}^{L} \gamma_l \tilde{p}_{jk,l}^2 =: w_0$, where $\tilde{p}_{jk,l}$ is given in (8a). To summarize, the objective (2a) subject to the equality constraints (2c) and (2d) can be written as an unconstrained convex quadratic program in the linearization parameters $\ell$,

$$\left. \begin{array}{l} \min\limits_{\ell} \; \mathbb{E}[(\mathsf{p}_{jk} - \hat{\mathsf{p}}_{jk})^2] \\ \text{s. t. (2c), (2d)} \end{array} \right\} = \min_{\ell} \ell^\top W \ell - 2w^\top \ell + w_0. \tag{13}$$

The "ingredients" $(W, w, w_0)$ are computed *after* the probabilistic power flow has been solved, as they require knowledge of all vectors of PCE coefficients $\tilde{P}_l$, $\tilde{Q}_l$, $\tilde{e}_l$, $\tilde{f}_l$ for $l = 0, \ldots, L$. Notice that $w_0$ is constant with respect to the linearization parameters $\ell$ and therefore only affects the optimal value.

### D. Computational Characteristics

As demonstrated, the linearization problem (2) can be decomposed into two parts: probabilistic power flow and an unconstrained optimization. Using PCE, the probabilistic power flow problem is rewritten as an *enlarged deterministic* power flow problem in terms of the PCE coefficients. Specifically, PCE-overloaded power flow is a square system that consists of $2n(L+1)$ equations in $2n(L+1)$ unknowns, namely, all the PCE coefficients from (8c) and (8d). Hence, all methods that solve deterministic power flow (e.g., Newton-Raphson) can, in principle, be applied to solve probabilistic power flow via PCE. The dimension of the PCE basis is given by $(L+1) = (N_\omega + N_d)!/(N_\omega N_d!)$, where $N_\omega$ is the number of distinct sources of uncertainties and $N_d$ is the maximum polynomial degree of the basis. For many applications, maximum degrees of $N_d = 2$ or $N_d = 3$ suffice to achieve sufficient numerical accuracy [14, 19]. The unconstrained convex optimization problem (13) poses no significant computational burden; in fact, it could be solved analytically.

## IV. Numerical Results

This section demonstrates the performance of the proposed expected-error-minimizing linearizations from (2). These linearizations are computed by implementing the algorithm from Section III in Julia with the solver Ipopt [20], and the packages JuMP [21] and PowerModels.jl [22].

For each example (IEEE 9-, 14- and 24-bus system), we solve an optimal power flow problem to obtain a nominal operating point. The active and reactive power injections at the nominal point are given by $p_i^{\text{nom}}$ and $q_i^{\text{nom}}$. We consider

$$w = \begin{bmatrix} \sum_{l=0}^{L} \gamma_l \left( g_{jk}(\tilde{e}_{j,l}^2 + \tilde{f}_{j,l}^2 - \tilde{e}_{j,l}\tilde{e}_{k,l} - \tilde{f}_{j,l}\tilde{f}_{k,l}) + b_{jk}(\tilde{e}_{j,l}\tilde{f}_{k,l} - \tilde{f}_{j,l}\tilde{e}_{k,l}) \right) \\ \sum_{l_1,l_2,l_3=0}^{L} \beta_{l_1 l_2 l_3} \Big( g_{jk} \Big( \tilde{e}_{j,l_1}\tilde{e}_{j,l_2} \begin{bmatrix} \tilde{P}_{l_3} \\ \tilde{Q}_{l_3} \end{bmatrix} + \tilde{f}_{j,l_1}\tilde{f}_{j,l_2} \begin{bmatrix} \tilde{P}_{l_3} \\ \tilde{Q}_{l_3} \end{bmatrix} - \tilde{e}_{j,l_1}\tilde{e}_{k,l_2} \begin{bmatrix} \tilde{P}_{l_3} \\ \tilde{Q}_{l_3} \end{bmatrix} - \tilde{f}_{j,l_1}\tilde{f}_{k,l_2} \begin{bmatrix} \tilde{P}_{l_3} \\ \tilde{Q}_{l_3} \end{bmatrix} \Big) + b_{jk} \Big( \tilde{e}_{j,l_1}\tilde{f}_{k,l_2} \begin{bmatrix} \tilde{P}_{l_3} \\ \tilde{Q}_{l_3} \end{bmatrix} - \tilde{f}_{j,l_1}\tilde{e}_{k,l_2}\tilde{P}_{l_3} \Big) \Big) \end{bmatrix} \quad (12)$$

where $\beta_{l_1 l_2 l_3} = \langle \psi_{l_1} \psi_{l_2}, \psi_{l_3} \rangle$

a range of operation around this nominal point defined by a specified probability distribution in terms of the active and reactive power injections at certain buses. In this paper, we consider uniform distributions:

$$\mathsf{P}_i \sim \mathbb{U}[p_i^{\text{nom}}(1 - \varepsilon/100), p_i^{\text{nom}}(1 + \varepsilon/100)], \quad (14a)$$

$$\mathsf{Q}_i \sim \mathbb{U}[q_i^{\text{nom}}(1 - \varepsilon/100), q_i^{\text{nom}}(1 + \varepsilon/100)]. \quad (14b)$$

The uncertainty is considered at PQ buses $i \in \mathcal{PQ}$ with a non-zero load. The random variables in (14) represent a uniform distribution with a fluctuation radius of $\varepsilon$ % around the nominal value, which can represent the size of the forecast uncertainty. The linearizations from (2) are compared to first-order Taylor expansions around the nominal operating point, $p_i^{\text{nom}}$, $q_i^{\text{nom}}$, whose errors are determined using Monte-Carlo simulations.

*1) Quality of Approximation:* For the IEEE 9-bus test case Figure 1 shows the characteristics of the linearization error as a function of the fluctuation radius $\varepsilon$ in (14) for both our linearizations ("PCE-Optimal") and the first-order Taylor expansions ("MC-Taylor"). The error predicted by the proposed method is very accurate in the sense that it is overlapping with the validation solution via Monte-Carlo ("MC-PCE"), see Figure 1. As expected, the optimal linearizations obtained using the proposed method outperform the first-order Taylor expansions. The improvement obtained can be quite significant for some lines, as is the case for the reactive power approximation of line #1, see Figure 1. The optimal linearization for this line has an error that is 5 MVAR lower than the Taylor expansion for an uncertainty radius of 100 %, which is significant compared to the 12.9 MVAR nominal flow. At the same time, the approximation errors are very small in other cases, indicating that Taylor approximations are appropriate for these lines.

*2) High-Voltage Solution:* Since the AC power flow equations are nonlinear and are known to admit multiple solutions, including so-called "low-voltage solutions" [23], we need to make sure that the PCE-overloaded power flow (8) represents the appropriate high-voltage solution for different uncertainty realizations. This is ensured in our numerical experiments by warm-starting the system of equations (8) with the nominal solution for the zero-order coefficients; the higher-order coefficients are initialized to zero. Also, Figure 1 and Figure 2 show that the error increases in a smooth manner from zero as the radius is increased, thus providing a-posteriori verification that the results obtained from solving the PCE-overloaded problem (8) indeed correspond to the high-voltage solutions.

*3) Comparing the Linearization Coefficients:* We compare the difference between the linearization coefficients obtained from the proposed optimal linearization and the first-order Taylor expansion. The root mean square (RMS) difference is plotted in Figure 2 as a function of the fluctuation radius $\varepsilon$. We observe that while the differences in the coefficients are rather small, the resulting improvement in the approximation errors can be quite significant, as shown in Figure 1.

*4) Comparison Across Test Cases:* We present the results of the optimal linearizations and the Taylor expansions for the IEEE 9-, 14- and 24-bus systems in Table I. There are several trends that generalize to all systems tested. First, there is a significant difference between expected squared error averaged over all lines ($e_{\text{avg}}$) and the largest expected squared error ($e_{\text{max}}$) for any line, suggesting that the Taylor approximation is reasonable for most of the lines except some critical lines where the optimal linearization shows significant improvements. Second, the approximation errors for reactive power flows are higher than the errors for active power flows. This is in agreement with the observations in [4] for the worst-case linearization error and is in accordance with the general intuition that reactive power tends to display higher levels of nonlinearity than active power.

*5) Computation Time:* The computation times for the two steps of the proposed method are given in the last column of Table I. Most of the time is spent solving the PCE-overloaded probabilistic power flow in (6). Once (6) is solved, computing an unconstrained convex quadratic program provides the optimal linearizations. This step is completed very quickly.

## V. Conclusion and Future Work

This paper proposes a method for computing power flow linearizations that are 1) *adaptive* to a specific system and operating range of interest, as defined by a specified probability distribution for the active and reactive power injections, and 2) *optimal* in the sense that they minimize the expected linearization errors relative to the nonlinear power flow equations. These optimal adaptive linearizations are computed using an approach based on Polynomial Chaos Expansion. Linearizations constructed for several test cases demonstrate the capabilities of this approach, such as expected linearization errors that are up to approximately a factor of two smaller than the errors resulting from a first-order Taylor expansion. Additionally, the error bounds provided by the proposed algorithm are validated using Monte Carlo sampling.

Our future work will improve the computational tractability of the approach with respect to the number of uncertainty sources (i.e. $> 10$). This may be achievable by characterizing which higher-order components of the PCE expansions are most relevant. We also plan to compare the performance of the expected-error-minimizing linearizations with alternatives, such as the adaptive linearizations proposed in [4, 9–11].

## References


[1] B. Stott, J. Jardim, and O. Alsaç. "DC Power Flow Revisited". In: *IEEE Trans. Power Syst.* 24.3 (Aug. 2009), pp. 1290–1300.

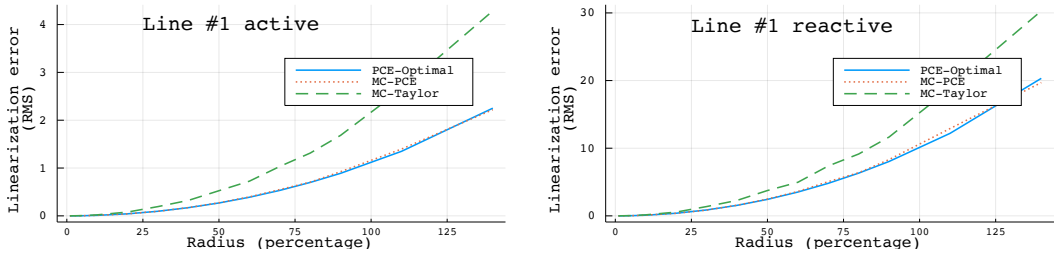


Figure 1. Root expected squared approximation error as a function of the fluctuation radius for line #1 in the IEEE 9-bus system.

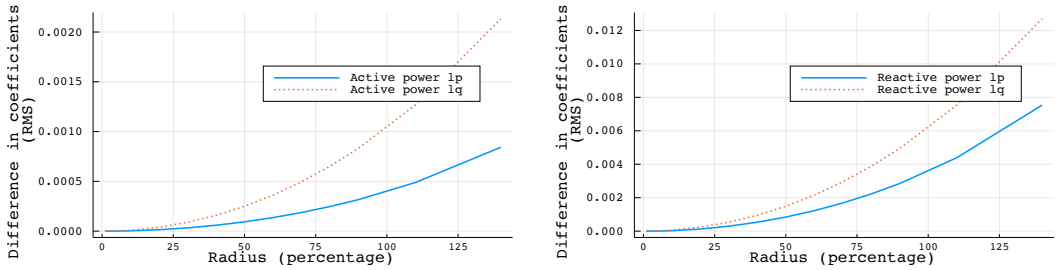


Figure 2. Root mean square (RMS) difference in linearization coefficients between PCE-optimal and first-order Taylor approximation as a function of the fluctuation radius for line #1 in the IEEE 9-bus system. Notice that this RMS is unitless because the linearization coefficients are ratios between power flows.

Table I

AVERAGE LINEARIZATION ERROR $e_{\text{avg}}$ AND MAXIMUM LINEARIZATION ERROR $e_{\max}$ IN (MW, MVAR) OVER ALL TRANSMISSION LINES.

| | | Radius = 10 % | | | | Radius = 50 % | | | | Radius = 90 % | | | | Radius = 140 % | | | | | |
|---|---|---|---|---|---|---|---|---|---|---|---|---|---|---|---|---|---|---|---|
| | IEEE | PCE | | Taylor | | PCE | | Taylor | | PCE | | Taylor | | PCE | | Taylor | | Time (sec.) | |
| | System | $e_{\text{avg}}$ | $e_{\max}$ | $e_{\text{avg}}$ | $e_{\max}$ | $e_{\text{avg}}$ | $e_{\max}$ | $e_{\text{avg}}$ | $e_{\max}$ | $e_{\text{avg}}$ | $e_{\max}$ | $e_{\text{avg}}$ | $e_{\max}$ | $e_{\text{avg}}$ | $e_{\max}$ | $e_{\text{avg}}$ | $e_{\max}$ | PCE | OPT |
| Active pow. | 9-bus | 0.00 | 0.01 | 0.00 | 0.02 | 0.00 | 0.27 | 0.00 | 0.53 | 0.04 | 0.89 | 0.05 | 1.68 | 0.81 | 2.25 | 1.25 | 4.28 | 3 | <1 |
| | 14-bus | 0.00 | 0.00 | 0.00 | 0.01 | 0.00 | 0.10 | 0.00 | 0.15 | 0.00 | 0.32 | 0.00 | 0.46 | 0.13 | 0.78 | 0.21 | 1.24 | 7 | <1 |
| | 24-bus | 0.00 | 0.01 | 0.00 | 0.03 | 0.00 | 0.32 | 0.00 | 0.78 | 0.01 | 1.07 | 0.02 | 2.58 | 0.94 | 2.78 | 1.58 | 6.57 | 25 | <1 |
| | | Radius = 10 % | | | | Radius = 50 % | | | | Radius = 90 % | | | | Radius = 140 % | | | | | |
| | IEEE | PCE | | Taylor | | PCE | | Taylor | | PCE | | Taylor | | PCE | | Taylor | | Time (sec.) | |
| | System | $e_{\text{avg}}$ | $e_{\max}$ | $e_{\text{avg}}$ | $e_{\max}$ | $e_{\text{avg}}$ | $e_{\max}$ | $e_{\text{avg}}$ | $e_{\max}$ | $e_{\text{avg}}$ | $e_{\max}$ | $e_{\text{avg}}$ | $e_{\max}$ | $e_{\text{avg}}$ | $e_{\max}$ | $e_{\text{avg}}$ | $e_{\max}$ | PCE | OPT |
| Reactive pow. | 9-bus | 0.00 | 0.10 | 0.00 | 0.15 | 0.01 | 2.44 | 0.01 | 3.75 | 0.22 | 8.04 | 0.34 | 11.66 | 5.12 | 20.3 | 7.90 | 30.30 | 3 | <1 |
| | 14-bus | 0.00 | 0.00 | 0.00 | 0.00 | 0.00 | 0.08 | 0.00 | 0.12 | 0.00 | 0.28 | 0.01 | 0.36 | 0.23 | 0.67 | 0.36 | 0.98 | 8 | <1 |
| | 24-bus | 0.00 | 0.04 | 0.00 | 0.08 | 0.00 | 1.13 | 0.00 | 2.09 | 0.03 | 3.77 | 0.05 | 6.97 | 2.77 | 9.77 | 4.65 | 18.10 | 25 | <1 |


[2] M. E. Baran and F. F. Wu. "Optimal Capacitor Placement on Radial Distribution Systems". In: *IEEE Trans. Power Del.* 4.1 (Jan. 1989), pp. 725–734.

[3] D. K. Molzahn and I. A. Hiskens. "A Survey of Relaxations and Approximations of the Power Flow Equations". In: *Foundations and Trends in Electric Energy Systems* 4.1-2 (Feb. 2019), pp. 1–221.

[4] S. Misra, D. K. Molzahn, and K. Dvijotham. "Optimal Adaptive Linearizations of the AC Power Flow Equations". In: *20th Power Syst. Comput. Conf. (PSCC)*. June 2018.

[5] L. A. Roald and G. Andersson. "Chance-Constrained AC Optimal Power Flow: Reformulations and Efficient Algorithms". In: *IEEE Trans. Power Syst.* 33.3 (May 2018), pp. 2906–2918.

[6] T. Mühlpfordt, T. Faulwasser, and V. Hagenmeyer. "A Generalized Framework for Chance-constrained Optimal Power Flow". In: *Sustainable Energy, Grids and Networks* 16 (2018), pp. 231–242.

[7] J. A. Martin and I. A. Hiskens. "Corrective Model-Predictive Control in Large Electric Power Systems". In: *IEEE Trans. Power Syst.* 32.2 (Mar. 2017), pp. 1651–1662.

[8] K. Dvijotham and D. K. Molzahn. "Error Bounds on the DC Power Flow Approximation: A Convex Relaxation Approach". In: *IEEE Conf. on Dec. and Contr.* Dec. 2016, pp. 2411–2418.

[9] J. R. Martí, H. Ahmadi, and L. Bashualdo. "Linear Power-Flow Formulation Based on a Voltage-Dependent Load Model". In: *IEEE Trans. Power Del.* 28.3 (July 2013), pp. 1682–1690.

[10] M. Hohmann, J. Warrington, and J. Lygeros. "Optimal Linearizations of Power Systems With Uncertain Supply and Demand". In: *IEEE Transactions on Power Systems* 34.2 (Mar. 2019), pp. 1504–1512.

[11] H. Ahmadi, J. R. Martí, and A. von Meier. "A Linear Power Flow Formulation for Three-Phase Distribution Systems". In: *IEEE Trans. Power Syst.* 31.6 (Nov. 2016), pp. 5012–5021.

[12] D. Xiu. *Numerical Methods for Stochastic Computations: A Spectral Method Approach*. Princeton University Press, 2010.

[13] T. J. Sullivan. *Introduction to Uncertainty Quantification*. Springer, 2015.

[14] T. Mühlpfordt, T. Faulwasser, and V. Hagenmeyer. "Solving Stochastic AC Power Flow via Polynomial Chaos Expansion". In: *IEEE Conf. on Control Applications*. Sept. 2016, pp. 70–76.

[15] T. Mühlpfordt, T. Faulwasser, L. Roald, and V. Hagenmeyer. "Solving Optimal Power Flow with Non-Gaussian Uncertainties via Polynomial Chaos Expansion". In: *IEEE Conf. on Dec. and Contr.* Dec. 2017, pp. 4490–4496.

[16] H. Sheng and X. Wang. "Applying Polynomial Chaos Expansion to Assess Probabilistic Available Delivery Capability for Distribution Networks with Renewables". In: *IEEE Trans. Power Syst.* 33.6 (Nov. 2018), pp. 6726–6735.

[17] A. J. Wood and B. F. Wollenberg. *Power Generation, Operation, and Control*. John Wiley & Sons, 2012.

[18] W. Gautschi. "On Generating Orthogonal Polynomials". In: *SIAM J. Sci. Stat. Comput.* 3.3 (1982), pp. 289–317.

[19] A. Engelmann, T. Mühlpfordt, Y. Jiang, B. Houska, and T. Faulwasser. "Distributed Stochastic AC Optimal Power Flow based on Polynomial Chaos Expansion". In: *American Control Conf.* 2018, pp. 6188–6193.

[20] A. Wächter and L. T. Biegler. "On the Implementation of a Primal-Dual Interior Point Filter Line Search Algorithm for Large-Scale Nonlinear Programming". In: *Math. Prog.*" 106.1 (2006), pp. 25–57.

[21] I. Dunning, J. Huchette, and M. Lubin. "JuMP: A Modeling Language for Mathematical Optimization". In: *SIAM Rev.* 59.2 (2017), pp. 295–320.

[22] C. Coffrin, R. Bent, K. Sundar, Y. Ng, and M. Lubin. "PowerModels.jl: An Open-Source Framework for Exploring Power Flow Formulations". In: *20th Power Syst. Comput. Conf. (PSCC)*. June 2018, pp. 1–8.

[23] A. Klos and A. Kerner. "The Non-Uniqueness of Load Flow Solution". In: *5th Power Syst. Comput. Conf. (PSCC)*. Cambridge, 1975, pp. 1–8.